EFFECT OF THE ELECTROMAGNETIC FIELD ON THE PHOTOISOMERIZATION OF THE RHODOPSIN MOLECULE

EFECTO DEL CAMPO ELECTROMAGNÉTICO SOBRE LA FOTOISOMERIZACIÓN DE LA MOLÉCULA RODOPSINA

J. Cerutti-Torres[a†], F. Rodríguez-Hernández[a], A. Martínez-Mesa[a], L. Uranga-Piña[a]

DynAMoS (Dynamical processes in Atomic and Molecular Systems), Facultad de Física, Universidad de La Habana, San Lázaro y L, La Habana 10400, Cuba; jcerutti@fisica.uh.cu[†]
† corresponding author

Recibido 22/3/2017; Aceptado 23/10/2017

Molecular photoisomerization is a process of configurational rearrangement induced by the action of electromagnetic radiation and whose efficiency can be controlled via the manipulation of the electric field that triggers the reaction. In the present work, we introduce a theoretical model for the isomerization process that incorporates the essential features of this phenomenon at the microscopic level. Two potential energy surfaces and two degrees of freedom are used to represent the active center of the molecule. The effect of the electric field on the overall dynamics is studied by considering different widths and shapes of the exciting field, within the electric dipole approximation. The rest of the system is modelled as a set of classical harmonic oscillators. The model reproduces previously reported experimental results on the isomerization yield upon instantaneous excitation and it predicts the behavior of the system under the action of laser pulses of finite duration.

La fotoisomerización molecular es un proceso de reordenamiento configuracional inducido por la acción de radiación electromagnética y cuya eficiencia puede controlarse mediante la manipulación del campo eléctrico que desencadena la reacción. En el presente trabajo se introduce un modelo teórico del proceso de isomerización que incorpora las características esenciales del fenómeno a nivel microscópico. Se utilizan dos estados electrónicos y dos modos nucleares para representar el centro activo de la molécula. El efecto del campo eléctrico sobre la dinámica se estudia a partir de la consideración de pulsos de diferentes formas y anchos temporales, dentro de la aproximación dipolar eléctrica. El resto de la molécula se modela como un conjunto de osciladores armónicos clásicos. El modelo reproduce resultados experimentales reportados previamente para la probabilidad de isomerización de la molécula rodopsina ante una excitación instantánea y predice el comportamiento del sistema bajo la acción de pulsos láser de duración finita.

PACS: Semiclassical theories in atomic physics (31.15.xg); Isomerization reactions (82.30.Qt); Ultrafast processes in femtochemistry (82.53.-k); Perturbation theory (31.15.xp); Molecular dynamics (31.15.xv)

I. INTRODUCTION

In the last decades, *cis* to *trans* isomerization has been the subject of a large number of experimental and theoretical works due to its importance in many chemical and biological processes [1–3]. Isomerization is a physical-chemical process in which the atoms forming a molecule change their equilibrium positions. *Cis* and *trans* configurations of the molecule usually exhibit notable differences in their physical and chemical properties. The energy required to activate the process is often provided by external perturbations. Typically, optical pulses are employed to excite the chromophore in the molecular system and to trigger the isomerization. In this case, the process is called photoisomerization.

The mechanism of human beings vision, the breaking of DNA strings and the activation of green fluorescent proteins are some examples of natural phenomena that involve photoisomerization [4–7]. Possible technological applications include nanometric motors and vehicles, molecular switches and memories [8–10]. The optimization of the wide family of possible applications demands the development and implementation of accurate microscopic descriptions of isomerization, and the possibility to control the outcome of the process by manipulating external parameters such as the width, shape and intensity of the optical pulses [11,12].

Different schemes based on the Classical Molecular Dynamics method are routinely used in a variety of dynamical problems with accurate results. Yet, molecular isomerization is an intrinsically quantum mechanical phenomenon that can not be adequately described using the laws of classical mechanics, as it exhibits pronounced non-adiabatic effects. A realistic description of the dynamics of these processes implies the simultaneous evolution of the system on different potential energy surfaces (PES). Nonetheless, a rigorous quantum-mechanic description of large polyatomic systems is infeasible at present due to its high computational cost.

Usually, a small part of the system (the active centre) reacts to the external perturbation, while the rest of the degrees of freedom behaves like a thermal bath (i.e., it takes part only in the redistribution of the excess energy deposited by the laser). The second group may be described using a less accurate methodology, for instance employing a classical or semiclassical approximation. This separation motivates the

development of hybrid quantum-classical models like the one introduced in this paper.

The present work focuses in the description of the interaction between a rhodopsin molecule and optical pulses of finite width using a hybrid quantum-classical approach for the description of the non-adiabatic dynamics. In the next section, the model Hamiltonian is presented as well as the methodology followed to compute the isomerization yields and the electronic and isomeric populations. Then, the results of the simulation of the isomerization dynamics are presented and discussed. Finally, some conclusions are drawn.

II. THEORETICAL MODEL

II.1. Unperturbed Hamiltonian

The main aspects of the dynamical response of the active centre of rhodopsin can be captured by a model Hamiltonian comprising two dimensionless coordinates: the torsion angle φ, that describes the twist around the C_{11}-C_{12} double bond [13], and q, which characterizes the collective vibrational motion of the active centre. The *cis* and *trans* configurations correspond to the ranges $-\frac{\pi}{2} < \varphi < \frac{\pi}{2}$ and $\frac{\pi}{2} < \varphi < \frac{3\pi}{2}$ of the isomerization coordinate, respectively.

Only two diabatic electronic states are involved in the process, the ground state $|0\rangle$ and the first excited state $|1\rangle$. The isomerization process takes place when the molecule is promoted to the excited state, it evolves on the excited PES, and eventually it passes through a conical intersection, where the wave function of the system splits in two separate wave packets each one approaching the *cis* or the *trans* configuration. The Hamiltonian for this two-state two-dimensional problem, in atomic units and in the diabatic representation, is written as [14]

$$\hat{H}_0 = \sum_{n,m=0,1} |n\rangle \left(\hat{T}\delta_{nm} + \hat{V}_{nm}\right) \langle m| \,, \tag{1}$$

where

$$\hat{T} = -\frac{1}{2I}\frac{\partial^2}{\partial\varphi^2} - \frac{\omega}{2}\frac{\partial^2}{\partial q^2}, \tag{2}$$

is the kinetic energy operator, I is the moment of inertia of the active centre, corresponding to the motion along the isomerization coordinate, and ω is the frequency of the collective mode q.

$$\begin{aligned} \hat{V}_{nn} &= E_n + (-1)^n \tfrac{1}{2}\tilde{V}_n(1-\cos\varphi) + \tfrac{\omega}{2}q^2 + \kappa q\delta_{n1}, \\ \hat{V}_{01} &= \hat{V}_{10} = \lambda q, \end{aligned} \tag{3}$$

are the potential energy surfaces and couplings in the diabatic representation. The numerical values of the parameters in equations (1)-(3) are chosen as in Ref. [15]: $I^{-1} = 4.84\cdot10^{-4}$ eV, $E_0 = 0$ eV, $E_1 = 2.48$ eV, $\tilde{V}_0 = 3.6$ eV, $\tilde{V}_1 = 1.09$ eV, $\omega = 0.19$ eV, $\kappa = 0.1$ eV y $\lambda = 0.19$ eV. This set of parameters reproduces the vertical excitation energies measured for a rhodopsin molecule in the *cis* and *trans* configurations. The physical interpretation of the quantities κ and λ follows from equation (3): the former represents the gradient along the q coordinate on the excited state, whereas the latter characterizes the strength of the non-adiabatic coupling between the electronic states.

II.2. Interaction with the electromagnetic field

If we consider a finite optical pulse excitation, there will be an additional coupling between the electronic states (besides the non-adiabatic terms in the Hamiltonian (1)) due to the field-matter interaction, influencing the exchange of population between these states. To take into account the effect of the finite electromagnetic pulses, it is necessary to add the field-molecule interaction to the unperturbed Hamiltonian. Within the dipole approximation

$$\hat{W}(t) = -E(t)\begin{pmatrix} 0 & \mu_{01} \\ \mu_{10} & 0 \end{pmatrix}. \tag{4}$$

The functions $\mu_{01} = \mu_{10} = \langle 0|\hat{\mu}|1\rangle$ denote the matrix elements of the transition dipole moment, which is chosen to be constant within the Franck-Condon approximation. The component of the external electric field along the molecular axis is written as

$$E(t) = E_0 f(t,\sigma) cos(\omega t) \,, \tag{5}$$

where the function $f(t,\sigma)$ is the envelope of the laser pulse of width σ. The frequency ω is chosen to be constant and its value is set to satisfy the resonance condition for the diabatic PES at the Franck-Condon point.

For simplicity, Gaussian profiles are the standard choice for the form of the pulse envelope in theoretical investigations of ultrafast photoinduced phenomena. Nevertheless, Gaussian functions can not accurately describe many realistic pulses which exhibit slowly falling wings. For that reason, in this work non-Gaussian forms for $f(t,\sigma)$ are also taken into account, e.g., $sech^2$ and Lorentzian functions [12]. In each case, the parameter σ stands for the full width at half maximum of the laser pulse. The numerical values $\sigma = 1, 5, 20, 50, 100, 200$ fs were considered for this parameter. They are representative of the range of interest in femtosecond spectroscopy applications.

In the majority of practical applications, the fields used have a relative small intensity to avoid the undesired occurrence of the so-called Rabi oscillations. This is why the field-molecule interaction $\hat{W}(t)$ described by Eq. (4) can be treated within the first-order perturbation theory.

II.3. Thermal bath

The Hamiltonian for the thermal bath is taken as

$$H_B = \sum_\alpha \frac{\omega_\alpha}{2}(x_\alpha^2 + p_\alpha^2) \,. \tag{6}$$

The quantities x_α and p_α are the canonical coordinates and momenta for each degree of freedom included in the

bath. They describe the motion of the atoms surrounding the active centre (the rest of the rhodopsin molecule). The magnitudes ω_α stand for the vibrational frequencies of these modes. Their values were chosen to reproduce the results of Raman spectroscopy measurements carried out on rhodopsin molecules [13].

II.4. System-bath dynamics

A detailed account of the methodology used to update the dynamical state of the system can be found elsewhere [14]. It involves the simultaneous solution of the time-dependent Schrödinger equation along the degrees of freedom of the active centre, and the Hamilton's equations of motion for the classical modes. The coupling between the quantum and the classical subsystems is described by the interaction Hamiltonian described in Ref. [3], which may be rewritten as

$$\hat{H}_{int} = \sum_{n=0,1} |n\rangle \sum_{\alpha} \left[g_{\varphi}^{(\alpha)} \cos^2\left(\frac{\varphi + n\pi}{2}\right) + \frac{g_q^{(\alpha)}}{2} q \right] x_\alpha \langle n| \,. \tag{7}$$

The coupling constants $g_\varphi^{(\alpha)}$ and $g_q^{(\alpha)}$ are chosen according to the Ohmic spectral bath densities

$$\frac{\pi}{2} \sum_{\alpha} g_s^{(\alpha)} \delta(\omega - \omega_\alpha) = \eta_s \omega e^{-\omega/\omega_{sc}} \qquad s = \{\varphi, q\} \,, \tag{8}$$

with the dimensionless coupling strengths $\eta_\varphi = 0.15$, $\eta_q = 0.10$, and the cut-off frequencies $\omega_{\varphi c} = 0.08$ eV, $\omega_{qc} = 0.20$ eV, respectively.

Electronic populations are computed by projecting the time-dependent wave function on the diabatic basis, while the isomeric populations are obtained by integrating the probability density over the ranges of the torsion angle φ corresponding to the *cis* and *trans* conformations.

III. RESULTS AND DISCUSSIONS

III.1. Instantaneous pulse

Figure 1 shows the time evolution of the two configurational states computed assuming an instantaneous excitation. At the beginning of the simulation ($t = 0$), the system is entirely in the *cis* configuration ($P_{cis}|_{t=0} = 1$), which reflects the initial condition imposed to the molecular wave packet. Since the laser pulse is assumed to be infinitely narrow, the promoted wave packet is an exact copy of ground state wave function, which is centred at the *cis* configuration. The populations change very rapidly, and around $t = 110$ fs the population of the excited state has decreased to 0.5. After some strong oscillations corresponding to the population transfer near the conical intersection, the values of the *cis-trans* populations get stabilized. At $t = 1ps$ the populations have reached their equilibrium values of $P_{cis}|_{t\to\infty} = 0.44$ and $P_{trans}|_{t\to\infty} = 0.56$. It can be noticed, that the probability for the molecule to return to its initial (*cis*) configuration is less than 50 %.

Figure 2 shows the time evolution of the diabatic electronic populations. The time origin is set to coincide with the instantaneous promotion of the wave packet to the excited state. Therefore, the initial population of the excited state is $P_1|_{t=0} = 1$. Conversely to the behaviour of the configurational states, the populations of the diabatic states change more slowly.

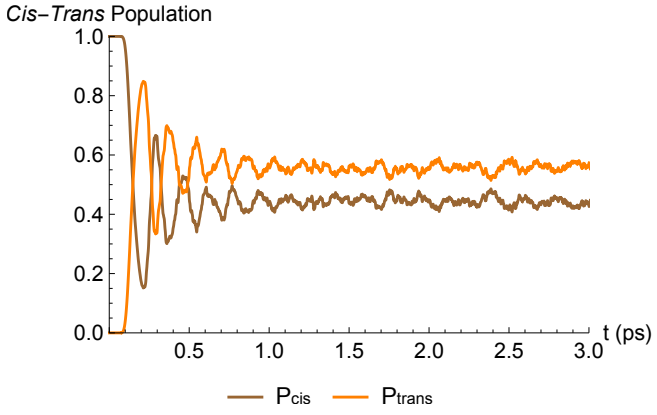

Figure 1. *Cis-trans* isomeric populations. At $t = 0$, the system is prepared in the *cis* configuration. The populations change very fast and after 1 ps they have reached their equilibrium values of $P_{cis}|_{t\to\infty} = 0.44$ and $P_{trans}|_{t\to\infty} = 0.56$.

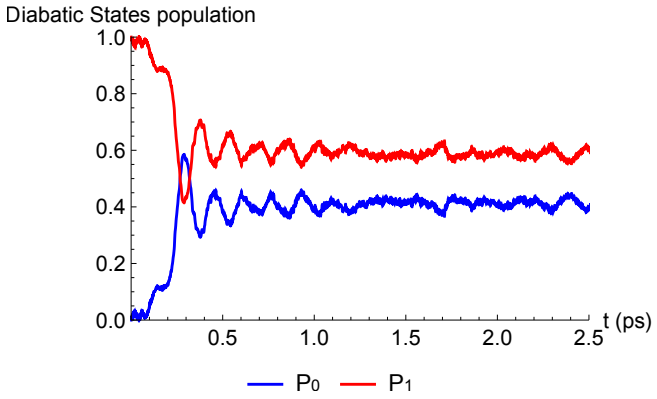

Figure 2. Diabatic electronic populations. In the beginning, the molecule is placed in the excited state. The populations change due to the coupling between the states near the conical intersection. The populations stabilize at $t = 0.5$ ps, reaching the values $P_1|_{t\to\infty} = 0.6$ and $P_2|_{t\to\infty} = 0.4$.

This is due to the fact that when the molecular wave packet reaches the *trans* configuration for the first time, it crosses the location of the conical intersection while it still remains on the excited diabatic PES. This process is dominated by the energetic difference between the hill and the valley on the excited diabatic state. The major part of the population transfer from the excited to the basic diabatic state takes place when the wave packet reaches the conical intersection for the second time, in this case with much less kinetic energy. The energy loss is dominated by the coupling terms between the active centre and the thermal bath. The populations stabilize after $0.5ps$ to the asymptotic values $P_1|_{t\to\infty} = 0.6$ and $P_2|_{t\to\infty} = 0.4$.

The isomeric populations in each adiabatic state was also analysed and it was compared with previously reported

results for $\delta(t)$-like excitations. The time scale of the process ($\sim$ 200 fs) is found to be in good agreement with experimental reports [15].

III.2. Effect of the shape of the envelope function and of the pulse width

Figure (3) shows the asymptotic values of the *trans* population for the three forms of the envelope function considered and for different widths of the laser pulse. It can be seen that, as a general trend, the three pulse shapes produce similar asymptotic values and they show a similar behaviour as a function of the pulse width. For the finite pulses, the *trans* population at long times increases as the value of σ gets larger. For every width, the lowest value of the isomerization probability corresponds to the Gaussian field. The asymptotic values of the *trans* population, computed for the Lorentzian and the $sech^2$ laser pulse shapes are similar to each other compared with the results of the calculations employing a Gaussian field.

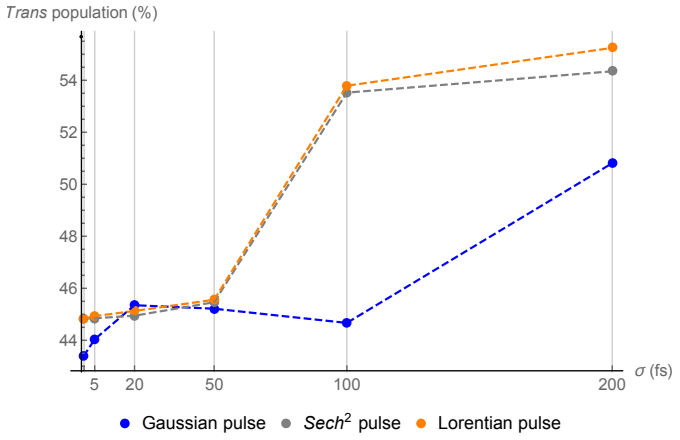

Figure 3. Asymptotic values of *trans* populations as a function of σ for the three envelopes shapes considered in this work. For the finite pulse widths, the *trans* populations increases with the value of σ.

IV. CONCLUSIONS

We studied the effect of a finite-width optical pulse in the photoisomerization of a rhodopsin molecule, in the weak-field regime and using first order perturbation theory. The *cis* to *trans* photoisomerization was investigated employing a hybrid quantum-classical model which describes quantum-mechanically the active centre of the molecule, while the rest of the system is treated as a bath of classical harmonic oscillators. The parameters of the model Hamiltonian were chosen to reproduce experimental data from Raman spectroscopy measurements performed on rhodopsin molecules. The time scale of the isomerization process obtained in the numerical simulations is in good agreement with previous experimental results reported in the literature.

We analysed the influence of the duration and the shape of the exciting pulse on the isomerization yield and on the electronic population dynamics. The results of the simulations point to the possibility to mildly control the non-adiabatic dynamics of the target molecule by tailoring the external electromagnetic field.

REFERENCES

[1] B. G. Levine, T. J. Martínez, Annu. Rev. Phys. Chem, 58, 613 (2007).

[2] M. Garavelli, P. Celani, F. Bernardi, M.A. Robb, M. Olivucci, J. Am. Chem. Soc, 119, 6891 (1997).

[3] W. Domcke, D. R. Yarkony, H. Köppel (Eds.), Conical Intersections: Electronic Structure, Dynamics and Spectroscopy. (World Scientific, Singapore 2004).

[4] D. Polli *et al.*, Nature 467, 440 (2010).

[5] G. Wald, Science. 162, 230 (1968).

[6] B. Juskowiak, A. Dominiaka, S. Takenakab, M. Takagib, Photochem. Photobiol. 74, 391 (2001).

[7] W. Weber, V. Helms, J.A McCammon, P.W. Langhoff, Proc. Natl. Acad. Sci. USA. 96, 6177 (1999).

[8] T. Raecker, N. O. Cartensen, B. Hartke, J. Phys. Chem. A. 116, 11241 (2012).

[9] W. R. Browne, B. L. Feringa, Nat. Nanotechnol. 1, 25 (2006).

[10] A.A. Beharry, G.A. Woolley, Chem. Soc. Rev. 40, 4422 (2011).

[11] A. H. Zewail, Adv. Chem. Phys. 101, 892 (1997).

[12] A. Martínez-Mesa, P. Saalfrank, J. Chem. Phys. 142, 194107 (2015).

[13] S. W. Lin, M. Groesbeek, I. van der Hoef, P. Verdegem, J. Lugtenburg, R. A. Mathies, J. Phys. Chem. B. 102, 2787 (1998).

[14] F. Rodríguez-Hernández, A. Martínez-Mesa, Ll. Uranga-Piña, Chem. Phys. Lett. 592, 18 (2014).

[15] X. Chen, V. S. Batista, J. Photochem. Photobiol., A. 190, 274 (2007).